Molecular Catalysis 587 (2025) 115470

Contents lists available at ScienceDirect

Molecular Catalysis

journal homepage: www.journals.elsevier.com/molecular-catalysis

Research Paper

Bioinspired copper corrole and porphyrin catalysts for oxidation and hydrocarboxylation of alkanes

Carla I.M. Santos [a,b,*], Vitor Rosa [c], M. Graça P.M.S. Neves [b], Alexander M. Kirillov [d], Marina V. Kirillova [d,*]

[a] Centro de Química Estrutural, Institute of Molecular Sciences, Departamento de Engenharia Química, Instituto Superior Técnico, Universidade de Lisboa, 1049–001 Lisboa, Portugal
[b] LAQV–REQUIMTE and Department of Chemistry, University of Aveiro, 3810–193 Aveiro, Portugal
[c] LAQV-REQUIMTE, Departamento de Química, Faculdade de Ciências e Tecnologia, Universidade NOVA de Lisboa, 2829-516 Caparica, Portugal
[d] MINDlab: Molecular Design & Innovation Laboratory, Centro de Química Estrutural, Institute of Molecular Sciences, Departamento de Engenharia Química, Instituto Superior Técnico, Universidade de Lisboa, Av. Rovisco Pais, 1049-001, Lisboa, Portugal

ARTICLE INFO

Keywords:
Bioinspired catalysis
Homogeneous catalysis
Copper catalysts
Corroles and porphyrins
Oxidation reactions

ABSTRACT

The development of novel bioinspired catalytic systems that are efficient in the mild oxidative transformation of alkanes remains an attractive research direction in the area of molecular catalysis. In the current study, three copper corrole/porphyrin complexes were synthesized, characterized, and evaluated as homogeneous catalysts in the oxidative transformation of cycloalkanes under mild conditions. New copper complexes of 5,10,15-tris(pentafluorophenyl)corrole and 5,10,15,20-tetrakis(pentafluorophenyl)porphyrin derivatives bearing a hydroxyethoxy unit were obtained via the controlled nucleophilic substitution of *para* fluorine atom with ethylene glycol. The model catalytic processes include: (i) the oxidation of cycloalkanes with H_2O_2 into a mixture of cyclic ketones and alcohols, and (ii) the hydrocarboxylation of cycloalkanes in the CO/$S_2O_8^{2-}$/H_2O system to generate cycloalkanecarboxylic acids as main products. Both model reactions occur under mild conditions (50−60 °C). Selectivity features, substrate and oxidant scope, and the effects of various reaction parameters were studied and discussed. The best catalysts were the copper corrole derivatives, the performance of which is slightly influenced by the presence of the ethylene glycol moiety. In particular, the copper(III) complex of 5,10,15-tris(pentafluorophenyl)corrole is an efficient catalyst for the mild oxidation and carboxylation of cycloalkanes. This work widens the types of Cu-based corrole/porphyrin derivatives that can be used as bioinspired catalytic systems.

1. Introduction

The development of novel bioinspired catalytic systems remains a challenge in modern catalysis. The synthesis of molecular catalysts based on the use of abundant and bioavailable metals along with simple, stable, and nontoxic ligands represents an appealing research approach [1–4]. In particular, Cu-based catalytic systems have gained a new impetus in recent years on account of the recognized bio- and redox activity of copper centers along with their coordination versatility and low cost [5–8]. However, some of the promising Cu-catalytic systems are sensitive to air and moisture and require complicated synthesis involving several reaction steps.

In this regard, attention has been given to metalloporphyrins, and more recently also to their metallocorrole analogues, as bioinspired catalysts in hydrocarbon oxidation reactions [9–13]. High flexibility of both tetrapyrrolic macrocycles toward structural modifications can explain their successful use in different fields, including medicine [14,15], photoactive materials [16,17], sensing [18–20] and catalysis [21–30].

The use of synthetic metalloporphyrins as catalysts in alkane and alkene oxidation reactions was firstly suggested by Groves and co-workers in 1979 [31]. They discovered that the role of cytochrome P450 in detoxification processes can be mimicked by synthetic metalloporphyrins. Since then, several research groups described various strategies to improve the catalytic activity of metalloporphyrin derivatives [32–34]. In general, these studies were mainly focused on Fe (III) and Mn(III) porphyrin complexes, whereas the porphyrin derivatives of Co, Cr, and Ru were less investigated. However, these

* Corresponding authors.
E-mail addresses: carla.santos@tecnico.ulisboa.pt (C.I.M. Santos), kirillova@tecnico.ulisboa.pt (M.V. Kirillova).

https://doi.org/10.1016/j.mcat.2025.115470

Available online 16 September 2025

compounds can act as catalysts to activate different oxygen donors (e.g., H_2O_2, alkyl hydroperoxides, peracids, sodium hypochlorite, or sodium periodate) [35]. During these studies, some porphyrinic ligands revealed stability limitations. For instance, Chang and co-workers demonstrated that in catalytic C–H oxidation reactions, the metalloporphyrins without substituents at the *meso* positions are not useful, because they undergo fast oxidative degradation [36]. Other studies showed that the introduction of electron-withdrawing and/or bulky substituents at the periphery of the porphyrin macrocycle (*meso* and/or *β*-pyrrolic positions) influences the electronic density around the metal ion and consequently the catalytic activity of the resulting metal complex [37–39]. Recently, Nakagaki and co-workers evaluated the catalytic efficiency of unsymmetric manganese(III) porphyrins, containing a different number of pentafluorophenyl and 3,4-dimethoxyphenyl substituents at the *meso* positions, in the oxidation reactions of cyclohexane with iodosylbenzene. These metalloporphyrins showed selectivity toward alcohol product in the cyclohexane oxidation, and the catalytic activity is increased when more pentafluorophenyl substituents are present in the porphyrins [40]. Porphyrin-based microporous network polymers were also described as active and recyclable heterogeneous catalysts for the oxidation of (*Z*)-cyclooctene and cyclohexane [41]. Other studies revealed that the immobilization of metalloporphyrins based on 5,10,15,20-tetrakis(pentafluorophenyl)porphyrin on supports (graphene, silica, and zinc oxide) may reduce catalyst decomposition and promote product formation [42–46].

In fact, the free base ligand, 5,10,15,20-tetrakis(pentafluorophenyl) porphyrin, represents a versatile platform for the design of new catalysts [47–49]. The fluorine atoms on the phenyl ring at the four *meso* positions can be readily substituted by nucleophiles, enhancing the stability and catalytic activity of porphyrins [50]. Castro et al. studied the catalytic efficiency and selectivity of a series of manganese(III) tetrakis (pentafluorophenyl)porphyrin derivatives bearing one to four ethylene glycol moieties in the oxidation of cyclohexane. Their results indicated that the catalytic performance depends on the number of ethylene glycol moieties present in the structure of porphyrin. All the substituted Mn(III) complexes were more efficient than the parent non-substituted porphyrin derivative [28].

Interestingly, the first application of metallocorroles as catalysts for the oxidation of hydrocarbons concerned an iron(III) complex of 5,10,15-tris(pentafluorophenyl)corrole, bearing C_6F_5 groups at the *meso* positions [51]. Other studies also involved the Mn(III) complex of 5,10,15-tris(pentafluorophenyl)corrole and its use as epoxidation catalyst [52].

Much less attention was given to the exploration of copper porphyrin and corrole complexes in the oxidation of saturated hydrocarbons. In the context of porphyrins, a modest catalytic activity of copper complexes encapsulated in the zeolite NaY was reported for cyclohexane oxidation with iodosylbenzene [53]. More recently, porphyrin copper complexes alone or combined with other metalloporphyrin derivatives were used in the preparation of porphyrin-based metal-organic framework materials, affording new heterogeneous catalysts for the oxidation of cycloalkanes with O_2 [54–56].

Hence, copper complexes of corroles and porphyrins represent a promising class of bioinspired catalysts that are still little explored in the oxidative functionalization of alkanes. The design of novel copper corrole and porphyrin catalysts for C–H functionalization reactions requires balancing electronic, steric, and redox properties. The macrocyclic ligand framework can stabilize high-valent copper-oxo or copper-superoxo intermediates, which are typically invoked as the active species in C–H bond cleavage. Being more electron-rich compared to porphyrins, corroles can enhance the electron-donating ability to copper and lower the energy barrier for generating high-valent states, and thus facilitate the oxidation reactions. Substituents on the macrocycle can be tuned to modulate electron density, enforce steric protection around the metal center to control substrate approach, and impart solubility. Important principles of catalyst design should also account for reversible redox behavior to allow catalytic turnover and introduction of optional peripheral groups that may mimic enzymatic environments to guide selectivity.

Following our general interest in the mild Cu-catalyzed oxidation [57,58] and carboxylation [59] of saturated hydrocarbons, the main aim of the present study consisted in investigating the catalytic efficiency of a new substituted Cu(III) corrole **Cu-C$_2$** bearing an ethylene glycol chain and to compare its efficiency with the non-substituted derivative **Cu-C$_1$**, as well as with the analogous porphyrin Cu(II) complex **Cu-P$_2$** (Scheme 1). When selecting these ligands, we considered their versatility for future immobilizations that may enable the preparation of heterogeneous catalytic systems.

The obtained Cu derivatives were tested as bioinspired catalysts in two model reactions: (i) mild oxidation of cycloalkanes with H_2O_2 to give a mixture of cyclic alcohols and ketones, and (ii) mild hydrocarboxylation of cycloalkanes with the $CO/H_2O//S_2O_8^{2-}$ system to produce cycloalkanecarboxylic acids as main products (Scheme 1). Substrate and oxidant scope, selectivity parameters, and the influence of various reaction conditions were studied and discussed in the present work.

2. Results and discussion

2.1. Synthesis of copper catalysts

In recent decades, various studies were devoted to the use of various metalloporphyrins as catalysts in the oxidation of hydrocarbons. However, the use of copper catalysts in this context is limited, although Cu complexes usually lead to good yields in the catalytic oxidation of (*Z*)-cyclooctene, cyclohexane, and heptane [60,61]. Castro and co-workers also demonstrated that copper complexes based on porphyrins are able to mimic the catecholase activity in the presence of hydrogen peroxide or air, affording a good conversion of catechols to the corresponding quinone derivatives [62,63]. The fact that the catalytic potential of corrole copper complexes is significantly less investigated prompted us to prepare and evaluate the activity of **Cu-C$_1$** and **Cu-C$_2$** (Cu corroles) and **Cu-P$_2$** (Cu porphyrin) in the oxidative functionalization of cycloalkanes (Scheme 1). In all the obtained compounds (**Cu-C$_1$**, **Cu-C$_2$**, and **Cu-P$_2$**), the copper centers are coordinated by four nitrogen atoms of the corrole or porphyrin core, likely forming distorted square pyramidal {CuN_4} environments, as previously described in other copper complexes with this type of ligands [64,65].

The target copper(III) complex **Cu-C$_1$** was obtained from 5,10,15-tris (pentafluorophenyl)corrole **C$_1$** in chloroform and in the presence of a moderate excess of $Cu(OAc)_2$ in methanol according to Scheme 2-Via A (see also Experimental Section and **Fig. S1A-S1C** in **SI**) [29]. In the synthesis of the mono-glycolcorrole **C$_2$**, the possibility of using microwave irradiation was explored for the first time (Scheme 2-Via A).

The substitution of the *p*-fluorine atoms in 5,10,15-tris(pentafluorophenyl)corrole by glycol units under classical heating conditions is usually carried out in the presence of sodium hydride (NaH) and ethylene glycol in refluxing tetrahydrofuran during 8 h. In this study, we found that the same reaction performed in dimethylsulfoxide, at an initial temperature of 150 °C and a pressure of 1 mbar under microwave irradiation, can afford the desired product **C$_2$** in 61 % yield in just 15 min. Copper insertion into **C$_2$** was performed with copper(II) acetate in $CHCl_3$ and MeOH (1:1) at room temperature for 1 h, resulting in the isolation of **Cu-C$_2$** in an almost quantitative yield (89 %). The structure of **Cu-C$_2$** was confirmed by NMR, UV–vis, fluorescence spectroscopy, and high-resolution mass spectrometry (**Fig. S2A-S2C, SI**). In particular, it was possible to assign in the ^{1}H NMR spectrum (**Fig. S2A**) the eight *β*-pyrrolic protons of the corrole core at lower field. In the aliphatic region, two triplets at δ ~4 and ~5 ppm were identified as the resonances of the four protons of the glycol chain. The ^{19}F NMR spectrum confirmed the loss of one *p*-F atom on the C_6F_5 unit at position 5 (**Fig. S2B, SI**).

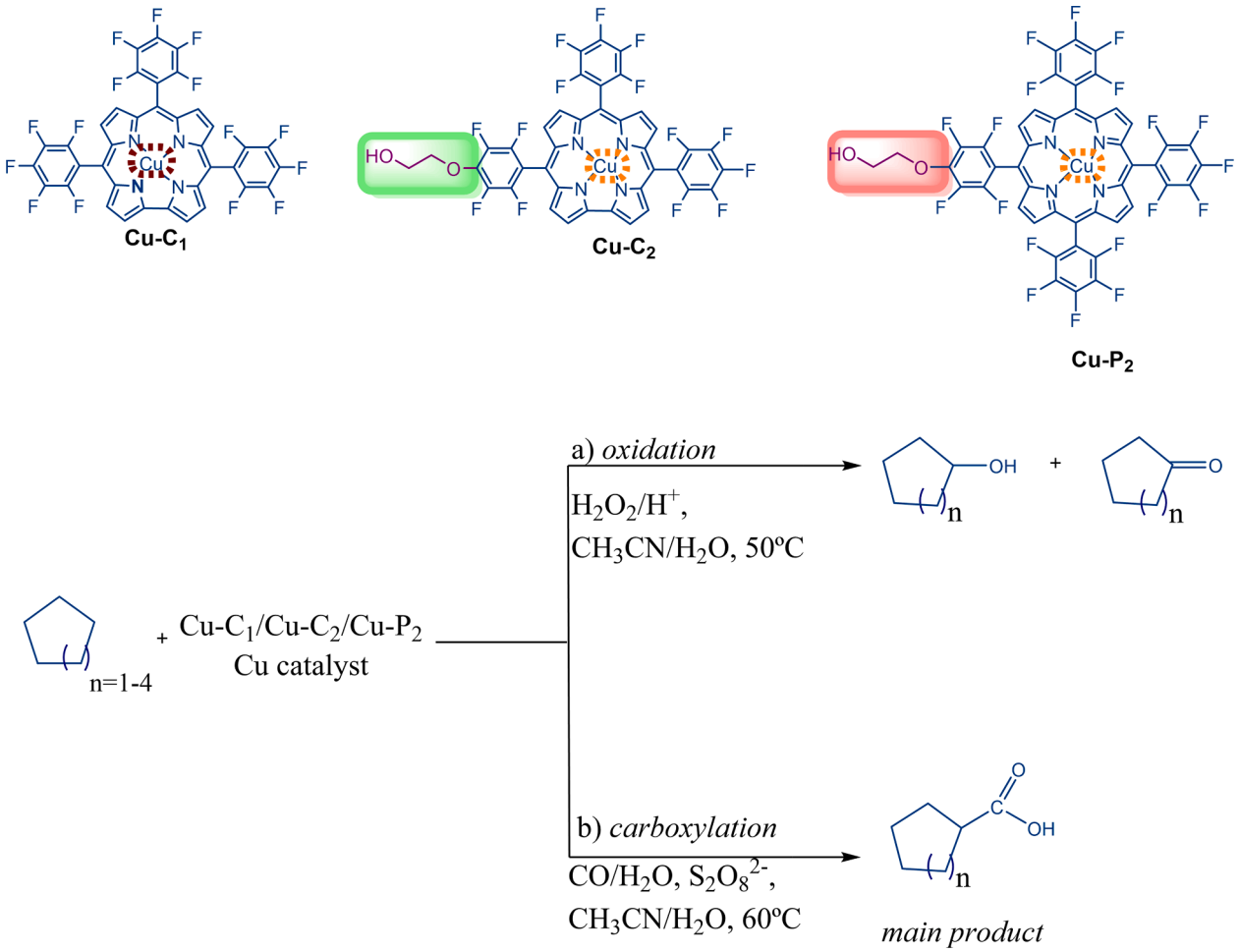

Scheme 1. Structures of Cu complexes and catalytic reactions explored: (a) oxidation and (b) carboxylation of C_5-C_8 cycloalkanes.

For the purpose of comparative studies, a glycol moiety was also introduced onto the *para*-position of one of the C_6F_5 units in the 5,10,15,20-tetrakis(pentafluorophenyl)porphyrin **P_1** under conventional heating conditions.28,65 The metallation of the resulting porphyrin **P_2** with copper(II) acetate was performed at 70 °C for 24 h affording the desired copper complex **Cu-P_2** in 98 % yield (Scheme 2-Via B). The structure of this complex was confirmed by FTIR, HRMS, UV–vis and fluorescence spectroscopy (see Experimental Section, **Figs. S3A-S3C** and **S4** in **SI**).

The FTIR spectra confirm the presence of the glycol (-OCH_2CH_2OH) group in the structure of the porphyrin macrocycle and also the metal insertion into the porphyrin ring [66,67]. The spectrum of porphyrin **P_2** shows typical bands of free-base porphyrins at 3322, 3106, 2964, 1649, and 1349 cm^{-1} corresponding to the stretching vibrations of -NH (pyrrole), -C-H- (phenyl), -C-H- (pyrrole), -C=C-, and -C-N- bonds, respectively [44,51]. In addition, the characteristic bands of the ethylene glycol group linked to the porphyrin can be seen at 1048 cm^{-1} (C-O-C symmetric axial deformation), 1165 cm^{-1} (C-O-C asymmetric axial deformation), 1433 cm^{-1} (CH deformation), and 3439 cm^{-1} (OH stretching). After the complexation to copper, the band of the NH (pyrrole) bond deformation (947 cm-1) disappeared, and a new band (1019 cm^{-1}) corresponding to the axial deformation of the Cu–N-pyrrole evolved (**Fig. S3A**). The analysis of the mass spectrum of **Cu-P_2** confirms the proposed structure, as evidenced by the presence of the $[M+H]^+$ ion at *m/z* 1078 (100 %) (**Fig. S3B**).

2.2. Catalytic oxidation of C_5-C_8 cycloalkanes

The catalytic efficiency of the obtained **Cu-C_1**, **Cu-C_2**, and **Cu-P_2** complexes was first evaluated at 50 °C in the mild oxidation of cyclohexane as a model substrate using aqueous H_2O_2 (50 %) as oxidant. The oxidation of cyclohexane in the presence of complex **Cu-C_2** affords a mixture of cyclohexanol (main product) and cyclohexanone (Scheme 3) and proceeds with an induction period of ~2 h (Fig. 1).

Following this induction period, the reaction leads to a total product yield of ~13 % (TON 26) based on cyclohexane after 6 h (**Table S1**, Fig. 1). In contrast to many other Cu-containing catalytic systems that are active only in the presence of an acid additive [58,68,69], catalyst **Cu-C_1** does not require any acid promoter. The presence of a small amount of promoter such as trifluoroacetic acid (TFA, 50 μmol) results in the decrease of the catalytic activity of **Cu-C_1** (Fig. 1a)

Under the same conditions, **Cu-C_2** exhibits a slightly inferior catalytic activity in comparison with **Cu-C_1** leading, after 6 h, to a total yield of cyclohexanol and cyclohexanone of ~9 % and TON of 18 (Fig. 1b, **Table S1**). The kinetic curve of product accumulation is very similar to that exhibited by **Cu-C_1**, revealing the same induction period of 2 h, and the same time (6 h) for completing the oxidation reaction. However, in this case and in contrast to **Cu-C_1**, the presence of TFA promoter has a slightly positive effect on the catalytic system, leading to a total yield of ~10 % (Fig. 1b, **Table S2**).

The activity of copper porphyrin complex **Cu-P_2** toward the oxidation of cyclohexane in the presence of H_2O_2 is lower than that of **Cu-C_1** and **Cu-C_2**, resulting in a total product yield of ~5 % and a longer 4 h induction period (**Fig. S5** and **Table S1**). The presence of TFA practically

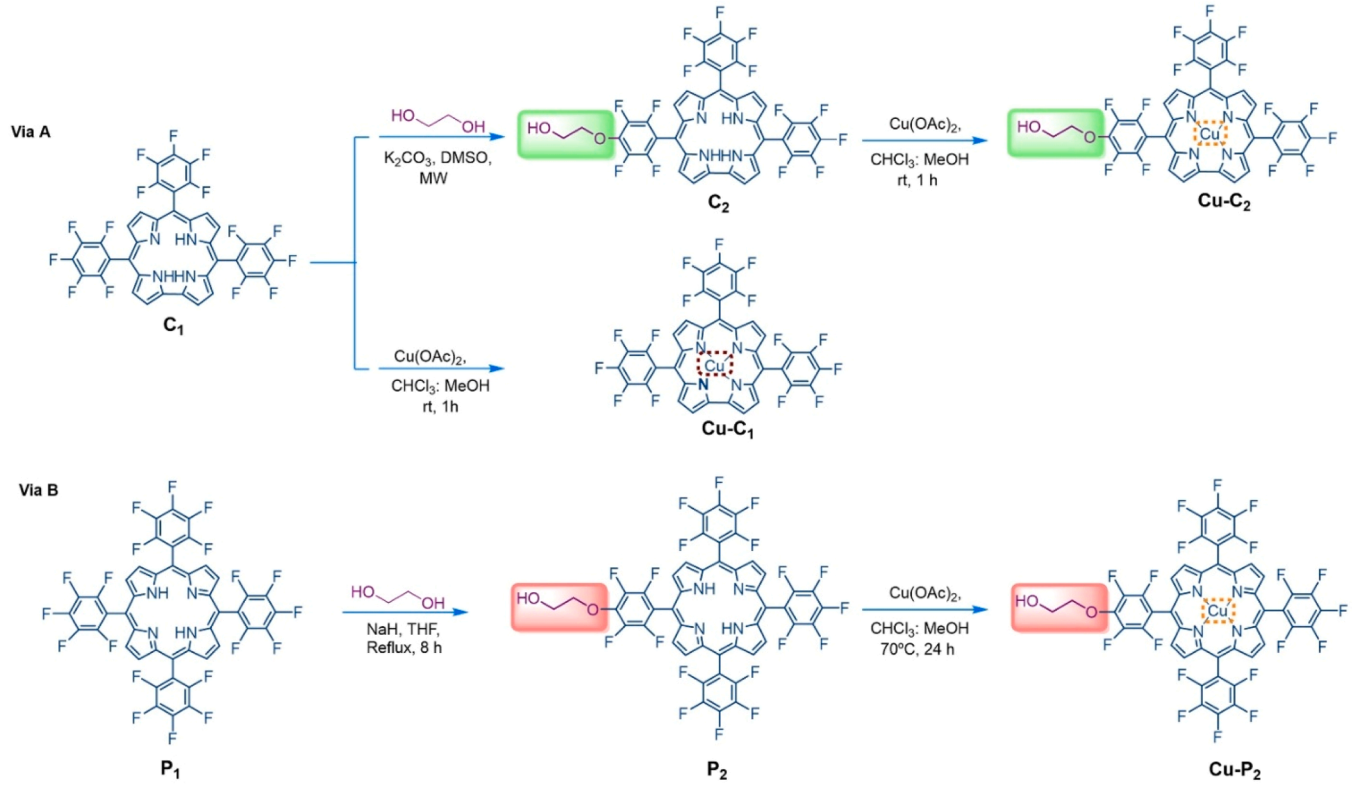

Scheme 2. Synthetic strategies for copper corroles **Cu-C$_1$** and **Cu-C$_2$** (Via A) and copper porphyrin **Cu-P$_2$** (Via B).

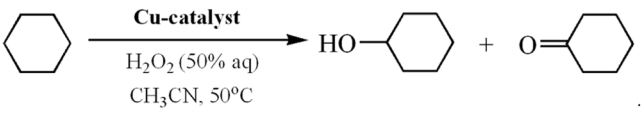

Scheme 3. Cu-catalyzed oxidation of cyclohexane into the mixture of cyclohexanol and cyclohexanone.

does not affect the kinetic curve of C_6H_{12} oxidation (**Table S2**).

After these assays, the catalytic activity of **Cu-C$_1$** was also tested in the oxidation cyclopentane, cycloheptane, and cyclooctane with H_2O_2 (Fig. 2). The results show a better performance of this catalytic system in the oxidation of C_7H_{14} (21 % product yield, TON 42) and C_8H_{16} (20 % yield, TON 40) when compared to cyclohexane. In the oxidation of cycloheptane and cyclooctane, the kinetic curves show similar shape and a 2 h induction period as observed in the case of C_6H_{12} oxidation.

To evaluate the role of oxidant, the oxidation of C_6H_{12} catalyzed by **Cu-C$_1$** was also studied in the presence of other oxidizing agents such as *tert*-butyl hydroperoxide (TBHP) and *tert*-butyl peroxybenzoate (TBPB) (Fig. 3). The results obtained show that these oxidations are faster but less efficient (ca. 7 % and 4 % total product yields in systems with TBPB and TBHP, respectively) in comparison to H_2O_2 (13 % product yield). In both cases, no induction period was observed (**Table S3**). A similar oxidant effect was observed in the presence of **Cu-C$_2$** (**Fig. S6**). In the

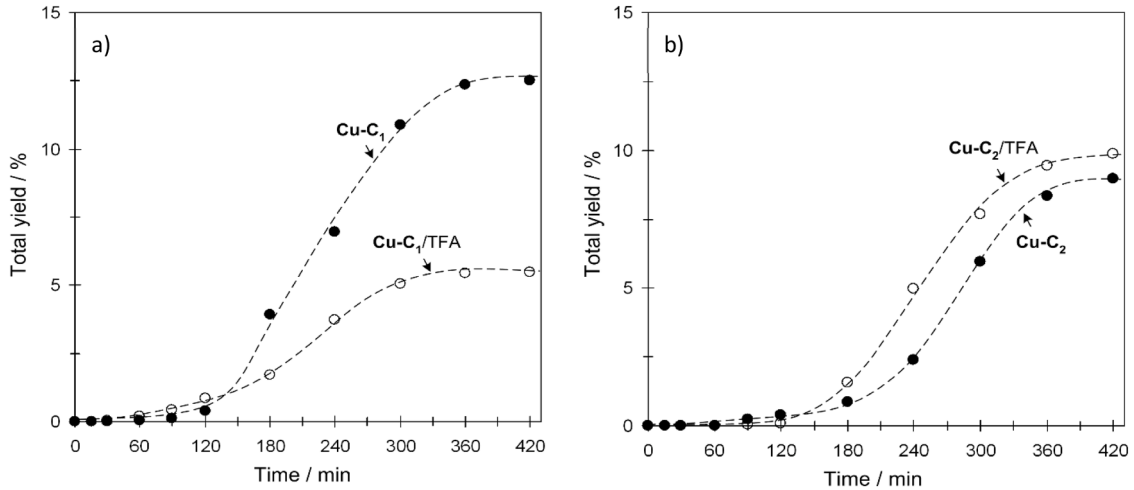

Fig. 1. Oxidation of cyclohexane by H_2O_2 to a mixture of cyclohexanol and cyclohexanone (total yield, %) catalyzed by **Cu-C$_1$** (a) or **Cu-C$_2$** (b) in the presence or in the absence of TFA promoter. Reaction conditions: catalyst (5.0 μmol), C_6H_{12} (1.0 mmol), TFA (if added, 50 μmol), H_2O_2 (50 % aq. 5.0 mmol), in acetonitrile solution at 50 °C.

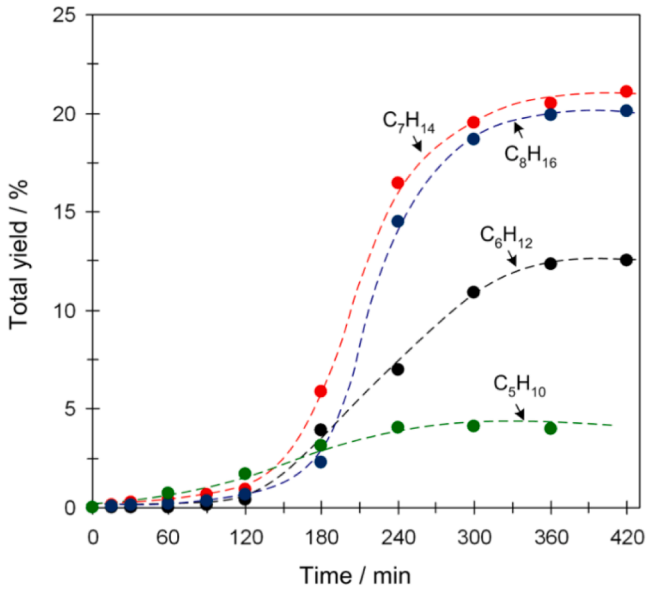

Fig. 2. Oxidation of C_5–C_8 cycloalkanes catalyzed by **Cu-C$_1$** in the presence of H_2O_2 to a mixture of the corresponding alcohols and ketones (total yield, %). Reaction conditions: catalyst **Cu-C$_1$** (5.0 μmol), cycloalkane (1.0 mmol), H_2O_2 (50 % aq. 5.0 mmol), in acetonitrile solution at 50 °C.

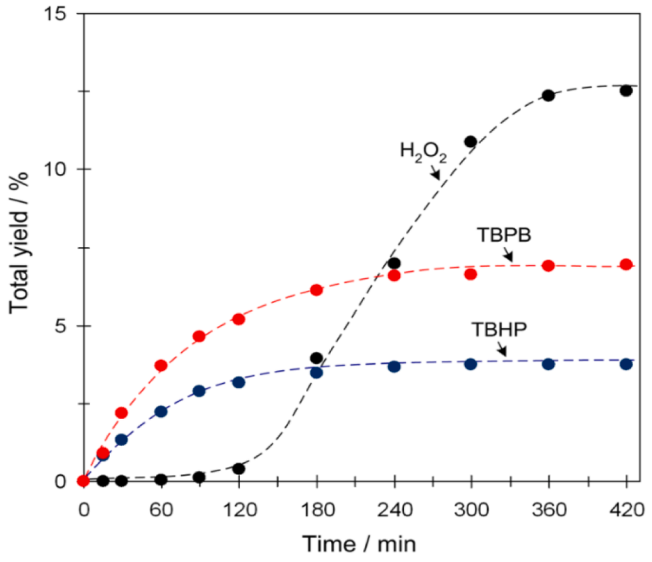

Fig. 3. Oxidant effect on the C_6H_{12} oxidation to a mixture of cyclohexanol and cyclohexanone (total yield, %) catalyzed by **Cu-C$_1$**. Reaction conditions: catalyst Cu-C_1 (5.0 μmol), C_6H_{12} (1.0 mmol), H_2O_2 (50 % aq. 5.0 mmol) or TBHP (70 % aq. 2.0 mmol) or TBPB (95 % aq. 2.0 mmol) in acetonitrile solution at 50 °C (in the case of H_2O_2) or 70 °C (in the case of TBHP or TBPB).

case of **Cu-P$_2$**, the presence of TBPB and TBHP leads to a considerable reduction of induction time (30 min vs. 4 h for H_2O_2). However, the total yields of the products are reduced (**Fig. S7**).

The oxidation of cyclohexane catalyzed by **Cu-C$_1$**, **Cu-C$_2$**, or by **Cu-P$_2$** was also performed under a nitrogen atmosphere, revealing almost similar product yields as in the reactions in the air atmosphere (conditions of Table S1). It should also be noted that molecular oxygen can also be easily formed from the Cu-promoted decomposition of H_2O_2 (catalase activity) present in excess in the reaction systems. To further clarify the role of O_2 (or oxygen in the air), the catalytic oxidation of cyclohexane in the presence of molecular oxygen was explored. For example, the oxidation of cyclohexane in the presence of O_2 excess (2 atm) catalyzed by **Cu-C$_1$** results in almost full suppression of its catalytic activity (only 0.9 % of the total oxidation products were obtained vs. 12.6 % under usual reaction conditions; conditions of **Table S1**). This is most likely associated with the inactivation of **Cu-C$_1$** in the presence of O_2 excess, as attested by a very fast transformation of the reaction solution from brown or light green to the dark green color. In contrast to **Cu-C$_1$**, the presence of O_2 in the cyclohexane oxidation catalyzed by **Cu-P$_2$** results in the enhancement of its catalytic activity. The total yield of oxygenated products increased from 5.4 % under usual reaction conditions (Table S1) up to 24 % in the presence of O_2 (2 atm). These findings reveal a distinct behavior of catalysts toward the presence of excess of oxygen.

Since copper corrole complexes can be photoactive, we decided to evaluate the performance of **Cu-C$_1$** in the oxidation of cyclohexane under light irradiation. These photocatalytic experiments were performed using an UV lamp (220 V, 40 W, wavelength: 330–400 nm). The results obtained in the C_6H_{12} oxidation under light irradiation and under normal light conditions are summarized in Fig. 4. It is clear that under the light irradiation, the oxidation proceeds much faster and the existing 2 h induction period is practically eliminated (**Fig. S8**). Interestingly, the maximum total yield of the products is not affected.

To gain further insights on the nature of the involved oxidizing species and on the reaction selectivity, the studies were extended to *n*-heptane (for regioselectivity), methylcyclohexane and adamantane (for site selectivity), and to *cis*- and *trans*-1,2-dimethylcyclohexane (for stereoselectivity). These experiments were conducted in the presence of **Cu-C$_1$** with H_2O_2 as oxidant (Table 1). The reaction with *n*-heptane proceeds without specific oxidation toward any secondary C-atom, considering that the relative normalized reactivities found for the hydrogen atoms at carbons 1, 2, 3, and 4 [C(1):C(2):C(3):C(4)] were 1:5:5:5. The relative normalized reactivity of the hydrogen atoms at primary, secondary and tertiary carbon atoms of methylcyclohexane (1°:2°:3°) was 1:6:31, while the reactivity at tertiary and secondary carbon atoms of adamantane (3°:2°) was 3.4. These values are not high and correspond to the powerful reaction species. Besides, the oxidations of both *cis*- and *trans*-isomers of 1,2-dimethylcyclohexane in the presence of **Cu-C$_2$**/H_2O_2 proceeded without any stereoselectivity. The obtained selectivity parameters (Table 1) are close to those early observed

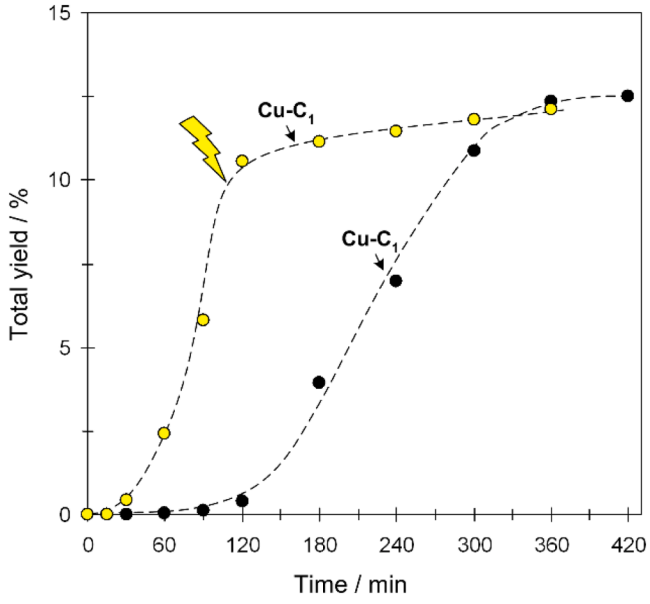

Fig. 4. Light irradiation effect on the oxidation of cyclohexane by H_2O_2 to the mixture of cyclohexanol and cyclohexanone (total yield, %) catalyzed by **Cu-C$_1$**. Reaction conditions: catalyst **Cu-C$_1$** (5.0 μmol), C_6H_{12} (1.0 mmol), H_2O_2 (50 % aq. 5.0 mmol), in acetonitrile solution at 50 °C. UV light lamp: 220 V, 40 W, 330–400 nm.

Table 1
Selectivity parameters in the Cu-catalyzed oxidation of linear and branched alkanes[a].

Selectivity parameter	Catalyst Cu-C_1
Regioselectivity	
C(1):C(2):C(3):C(4)[b] (*n*-C_7H_{16})	1:5:5:5
Site selectivity	
1°:2°:3° (methylcyclohexane)[c]	1:6:31
3°:2° (adamantane)[d]	3.4
Stereoselectivity	
trans/cis (*cis*-1,2-dimethylcyclohexane)[e]	0.9
trans/cis (*trans*-1,2-dimethylcyclohexane)[e]	0.9

[a]Reaction conditions: Catalyst **Cu-C_1** (5.0 μmol), alkane (1.0 mmol), H_2O_2 (5.0 mmol), CH_3CN up to 2.5 mL of total volume, 5 h, 50 °C. All parameters were calculated based on the ratios of isomeric alcohols. The calculated parameters were normalized, i.e., recalculated taking into account the number of H atoms at each carbon atom. [b]Parameters C(1):C(2):C(3):C(4) are the relative reactivities of H atoms at carbons 1, 2, 3 and 4 of the *n*-heptane chain. [c]Parameters 1°:2°:3° are the relative normalized reactivities of H atoms at primary, secondary and tertiary carbons of methylcyclohexane. [d]Parameters 3°:2° are the relative normalized reactivities of H atoms at tertiary and secondary carbons of adamantane. [e]Parameter *trans/cis* is determined as the ratio of the formed tertiary alcohol isomers with mutual *trans* and *cis* orientation of the methyl groups.

for related systems, including Cu-based catalytic systems that operate with hydroxyl radicals [57–59]. The involvement of hydroxyl radicals as main oxidizing species was further confirmed by ESI-MS investigation of catalyst **Cu-C_1** (**Fig. S9**). In fact, a major fragment in the mass spectrum (positive mode) is associated with a radical cation of **Cu-C_1** at *m/z* 855.9751. After the addition of H_2O_2, it is possible to observe the formation of an adduct at *m/z* 872.0289, which corresponds to (OH)**Cu-C_1^+** species.

The stability of **Cu-C_1** during the cyclohexane oxidation was investigated by UV–Vis spectroscopy. The interaction between **Cu-C_1** and cyclohexane, in the presence of H_2O_2 at 50 °C, was accompanied by changes in the UV–vis spectrum of **Cu-C_1** and by the color of the reaction solution. Initially, the **Cu-C_1** complex exhibited an absorption maximum known as the Soret band near 410 nm, along with two Q-bands at 565 and 600 nm, and a brown color (**Fig. S10**). After the addition of H_2O_2 the Soret band was split into two bands at 407 and 428 nm with a relatively large absorption at 585 nm, and the color of the solution changed to green. This behavior is typical for the formation of a cation radical [70], which is also supported by the mass spectrometry data. At the end of the reaction, the splitting of the Soret band was still observed, although the absorption became weaker, and the solution changed to a pale beige color. These final observations may be attributed to structural changes in the catalyst under the reaction conditions [71]. As typically observed in homogeneous catalysis, the present copper catalysts are not completely intact in the reaction systems containing oxidant, as thus act as precursors for copper-based catalytically active species.

2.3. Catalytic hydrocarboxylation of C_5-C_8 cycloalkanes

The activity of complex **Cu-C_1** was also evaluated in the hydrocarboxylation of C_5−C_8 cycloalkanes. In this reaction, there is a direct addition of carboxylic acid group COOH to alkane in the presence of CO, H_2O, and $K_2S_2O_8$, leading to the formation of monocarboxylic acids as main products (Scheme 4 and Table 2).

The results summarized in Table 2 show that the best reactivity is exhibited by C_6H_{12}, followed by C_5H_{10}, C_7H_{14}, and C_8H_{16}. When using

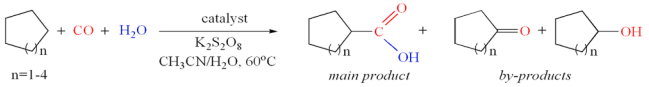

Scheme 4. Cu-catalyzed carboxylation of C_5−C_8 cycloalkanes with CO/$K_2S_2O_8$/H_2O system.

cyclohexane substrate, cyclohexanecarboxylic acid $C_6H_{11}COOH$ was formed in a considerable yield (31 % based on alkane), followed by minor amounts of cyclohexanone (0.6 %) and cyclohexanol (0.3 %), with a total TON of 64. Cyclopentane carboxylation affords cyclopentanecarboxylic acid in 25 % yield (total TON of 55), along with minor amounts of cyclopentanone (1.4 %) and cyclopentanol (0.7 %). The carboxylation of C_7H_{14} leads to the formation of 21 % of $C_7H_{13}COOH$, 4.2 % of cycloheptanone and 2.5 % of cycloheptanol. In the case of cyclooctane, the carboxylation reaction proceeds less efficiently, and the oxidation is more pronounced in comparison with other cycloalkanes. As a result, the cyclooctanecarboxylic acid (10.1 % yield) is formed as a major product, along with cyclooctanone (6.6 %) and cyclooctanol (6.1 %). The formation of oxidation products in higher amounts in the case of cyclooctane might be associated with an increased stability of cyclooctyl radicals that are more prone to undergo oxidation rather than carboxylation.

2.4. Proposed mechanism

Based on the obtained experimental evidence including selectivity parameters summarized in Table 1, as well as prior literature background on copper-catalyzed oxidation and carboxylation of alkanes [57–59,68], there is a clear evidence for free-radical mechanisms in oxidative functionalization of alkanes catalyzed by the present type of corrole/porphyrin copper complexes. The main mechanistic steps are depicted in Scheme 5 for cyclohexane as a model substrate.

In brief, the oxidation of cyclohexane (CyH) involves the generation of HO• radicals via interaction of Cu catalyst with hydrogen peroxide (step 1.1), the reaction of hydroxyl radicals with cyclohexane results in the abstraction of H atom and formation of cyclohexyl radical Cy• (step 1.2), the interaction of Cy• with O_2 (from air or formed from H_2O_2 decomposition) to form CyOO• radical (step 1.3), the transformation of CyOO• to cyclohexylperoxide anion (step 1.4), the formation of CyOOH as a primary intermediate product (step 1.5), and decomposition of cyclohexyl hydroperoxide (CyOOH) into the final cyclohexanol CyOH and cyclohexanone Cy'=O products (step 1.6).

The main steps of the carboxylation reaction include the homolysis of persulfate anion $S_2O_8^{2-}$ to give sulfate radical SO_4•$^-$ (step 2.1), the abstraction of a hydrogen atom by the reaction of SO_4•$^-$ with cyclohexane to give cyclohexyl radicals Cy• (step 2.2), the carbonylation of Cy• by carbon monoxide to generate acyl radicals CyCO• (step 2.3), the formation of $CyCO^+$ upon oxidation of acyl radicals involving copper-based redox couple (step 2.4), and the hydrolysis of $CyCO^+$ to obtain the final carboxylic acid product (step 2.5).

3. Conclusions

In the present study, new corrole copper complexes **Cu-C_1** and **Cu-C_2** were successfully prepared and fully characterized. Their efficiency as bioinspired catalysts was evaluated in the oxidative functionalization of cycloalkanes and compared with that of a porphyrinic copper complex

Table 2
Mild Cu-catalyzed carboxylation of C_5-C_8 cycloalkanes with Cu-C_1/CO/$K_2S_2O_8$/H_2O system[a].

Alkane RH	Product Yield, %[b] R-COOH	R=O	ROH	Total Yield, %	TON[c]
C_5H_{10}	25.2	1.4	0.7	27.3	55
C_6H_{12}	31.0	0.6	0.2	31.8	64
C_7H_{14}	21.2	4.2	2.5	27.9	56
C_8H_{16}	10.1	6.6	6.1	22.8	46

[a] Reaction conditions: cycloalkane: C_5H_{10}-C_8H_{16} (1.0 mmol), catalyst **Cu-C_2** (5 μmol), H_2O (2 mL)/MeCN (4 mL), CO (20 atm), $K_2S_2O_8$ (1.5 mmol), 4 h, 60 °C, stainless steel autoclave (20 mL). [b]Yields are based on cycloalkane: (moles of products per mol of alkane) × 100 %. [c]Moles of carboxylation products per mol of catalyst.

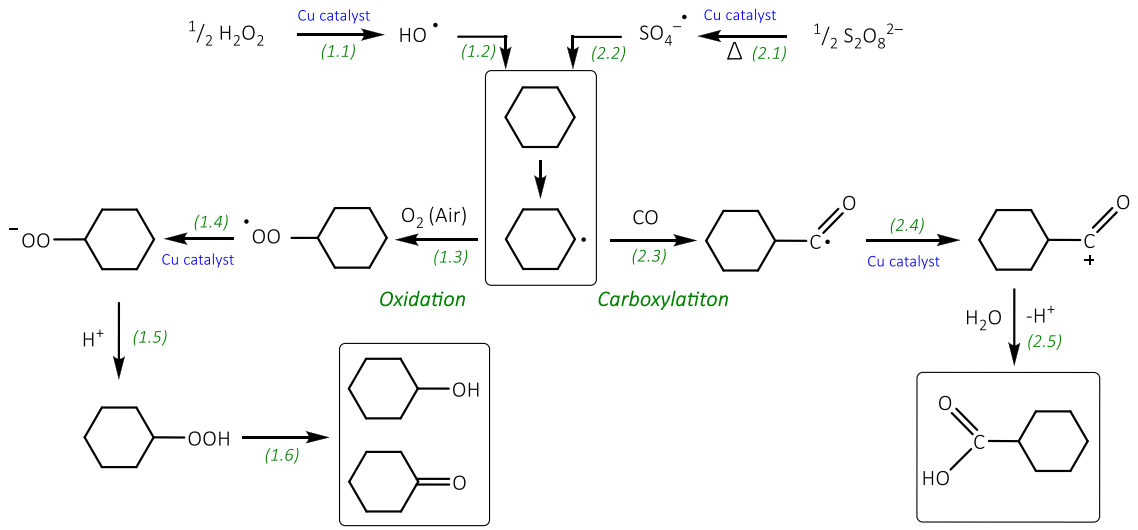

Scheme 5. Proposed reaction mechanism for oxidation (pathways 1.1–1.6) and carboxylation (pathways 2.1–2.5) of cyclohexane as a model substrate.

Cu-P$_2$. For the synthesis of corrole **C$_2$** with a glycol unit, we found that the use of microwave irradiation allowed to reduce the reaction time from 8 h under conventional heating to 15 min, and increase the reaction yield.

In addition to enlarging the family of copper corrole/porphyrin complexes, the obtained compounds show various catalytic features in two model reactions studied. These include (i) the mild oxidation of cycloalkanes with hydrogen peroxide to give cyclic alcohols and ketones, and (ii) the hydrocarboxylation of cycloalkanes with CO, H_2O and persulfate oxidant into the corresponding cycloalkane carboxylic acids. As typically observed in homogeneous catalysis, the present copper catalysts are not completely intact in the reaction systems containing oxidant, as thus act as precursors for copper-based catalytically active species. Further research on the heterogenization of copper corrole/porphyrin complexes to improve stability and enable their recyclability should be pursued.

Considering the inertness of alkanes and the mild reaction conditions (H_2O-CH_3CN medium, 50−60 °C), the obtained catalyst turnover numbers (TONs) and product yields are appreciable in the field of mild oxidative transformation of alkanes. For example, an industrial oxidation of C_6H_{12} into cyclohexanol and cyclohexanone (known as KA oil and used as intermediate in nylon-6 production) relies on a homogeneous cobalt catalyst and requires harsher conditions (150−160 °C), resulting in generally low total product yields (5−10 % based on cyclohexane) [72,73]. Although the direct comparison of the observed catalytic activity with other corrole/porphyrin catalysts is difficult to realize due to a limited amount of data available and distinct reaction conditions used (e.g., different oxidants and oxidant-to-substrate molar ratios), the present catalytic systems show the activity that is superior or comparable to other Cu-based catalysts in oxidative functionalization of cycloalkanes [57–59,68]. Notably, the main advantages of the developed herein systems and reaction protocols consist of low reaction temperatures, high selectivity toward main products, and the additive-free conditions (for example, no need for acid promoter in cycloalkane oxidation).

In the oxidation of cyclohexane, the corrole complexes **Cu-C$_1$** and **Cu-C$_2$** showed a better performance when compared with the porphyrin complex **Cu-P$_2$**. The performance of **Cu-C$_1$** was even better when the studies were extended to C_7H_{14} and C_8H_{16} substrates, leading to the total product yields of ~20 %. Hydrogen peroxide was the best oxidant in these oxidative reactions. The elimination of the induction period (~2 h) by using the UV light irradiation represents an interesting feature and corroborates the involvement of hydroxyl radicals as oxidizing species. This conclusion on a radical type process is further confirmed by evaluating the selectivity parameters. The results obtained in the hydrocarboxylation of cycloalkanes in the presence of **Cu-C$_1$** were also promising, with the best performance observed when using C_6H_{12}, followed by C_5H_{10}, C_7H_{14}, and C_8H_{16}.

The obtained copper compounds can also be considered as bio-inspired catalytic systems with relevance to Cu-containing oxidizing enzymes, including the particulate methane monooxygenase (*p*MMO), which can catalyse the oxidation of inert C−H bonds in alkanes and other substrates. Additional studies dealing with the synthesis of novel copper corrole/porphyrin catalysts and their immobilization into various supporting materials are in progress.

4. Experimental

4.1. Synthesis of copper complexes

Synthesis and analytical data of corrole derivatives. The free-base 5,10,15-tris(pentafluorophenyl)corrole **C$_1$** was synthesized as described in the literature [74]. Its purity was confirmed by thin layer chromatography (TLC) and ^{1}H NMR spectroscopy. 5,10,15-Tris-(pentafluorophenyl)corrolatocopper(III) **Cu-C$_1$** was prepared using copper(II) acetate and following the procedure reported by Cao *et al.* (Scheme 1-Via A) [75].

Analytical data for **Cu-C$_1$** (Figs. S1A-S1D): ^{1}H NMR (500 MHz, $CDCl_3$), δ (ppm) and *J* (Hz): 8.58–8.62 (m, 4H, H-β), 8.77 (d, *J* = 4.8 Hz, 1H, H-β), 8.80 (d, *J* = 5.0 Hz, 1H, H-*β*), 9.14–9.10 (m, 2H, H-β). ^{19}F NMR (282 MHz, $CDCl_3$), δ (ppm) and *J* (Hz): −136.69 (dd, *J* = 23.1, 7.1 Hz, 4F, F*orto*), −135.91 (dd, *J* = 22.0, 7.3 Hz, 2F, F*orto*), −151.83 to −151.98 (m, 3F, F*para*), −160.36 to −162.58 (m, 6F, F*meta*). HRMS-ESI (+), $CHCl_3$: *m/z* calculated for $C_{37}H_8CuF_{15}N_4$ $[M]^{+\cdot}$ 855.976821; found: 855.97999. UV–vis (CH_2Cl_2), λ_{max} in nm (log ε): 410 (4.51), 419 (4.08), 565 (3.79), 608 (3.42). FTIR (KBr, cm^{-1}): 3314 (m, O-H stretching), 3038 (w), 3021 (w, C-H pheny), 1604 (m, C=C stretching), 1583 (m), 1477 (m), 1446 (m), 1349 (s), 1182 (m, C-O-C asymmetrical axial deformation), 1016 (m, C-O-C, symmetric axial deformation), 974 (s), 798 (s), 703 (s).

Corrole **Cu-C$_2$** was synthetized under microwave irradiation. Ethylene glycol (2.09 mmol, 130 mg) and K_2CO_3 (0,0625 mmol, 8.7 mg) were added to a solution of 5,10,15-tris(pentafluorophenyl)corrole **C$_1$** (0031 mmol, 25.0 mg) in DMSO (1 mL) and transferred into a glass reactor. The reaction was carried out during 15 min under the microwave irradiation conditions (150 °C, 1 mbar pressure). After reaction, the solvent was evaporated under reduced pressure and the reaction mixture was washed with water (10 mL) and extracted with CH_2Cl_2 (15

mL). The organic phase was collected, dried over Na_2SO_4, and the solvent was removed under reduced pressure. Preparative TLC was used to purify the crude solid, using a mixture of chloroform-methanol (9:1) as the mobile phase. The purification allowed to separate the starting corrole **C_1** (first fraction) from the mono-substituted corrole **C_2** (second fraction), which was isolated in 61 % (15.8 mg) yield.

Subsequently the free-base corrole **C_2** was metallated with copper(II) acetate, by modifying the conventional methodology reported by Cao et al. [32] Briefly, **C_2** (0.02 mmol, 17,2 mg) was dissolved in 15 mL of a $CHCl_3$:MeOH (1:1) mixture and an excess of copper(II) acetate (0.06 mmol, 11,3 mg) was added. The resulting reaction mixture was stirred for 1 h at room temperature. Then, the solvent was removed under reduced pressure and the resulting solid was washed thoroughly with water to remove the excess of Cu(II) acetate to give **Cu-C_2** in 89 % (16.2 mg) yield (**Fig. S2A-S2D**).

Analytical data for **Cu-C_2**: ^{1}H NMR (300 MHz, $CDCl_3$), δ (ppm) and *J* (Hz): 1.55 (broad s, 1H, OH), 4.09 (t, $J = 4.3$ Hz, 2H, CH_2), 4.64 (t, $J = 4.3$ Hz, 2H, CH_2), 8.58–8.56 (m, 4H, H-β), 8.77 (d, $J = 4.5$ Hz, 1H, H-β), 8.82 (d, $J = 4.5$ Hz, 1H, H-β), 9.10–9.06 (m, 2H, H-β). ^{19}F NMR (282 MHz, $CDCl_3$), δ (ppm) and *J* (Hz): −133.61 (dd, $J = 23.2$, 7.1 Hz, 2F, F*orto*), −134.14 (dd, $J = 23.2$, 8.6 Hz, 2F, F*orto*), −135.87 (dd, $J = 22.0$, 7.4 Hz, 2F, F*orto*), −148.82 (t, $J = 22.5$ Hz, 1F, F*para*), −149.36 (t, $J = 22.5$ Hz, 1F, F*para*), −153.36 (dd, $J = 23.2$, 8.6 Hz, 2F, F*meta*), −157.99 (dt, $J = 22.0$, 7.4 Hz, 2F, F*meta*), −158.44 (dt, $J = 23.2$, 7.3 Hz, 2F, F*meta*). HRMS-ESI(+), $CHCl_3$: *m/z* calculated for $C_{39}H_{13}CuF_{14}N_4O_2$ $[M]^{+\cdot}$: 898.014384; found: 898.01054. UV–vis (CH_2Cl_2), λ_{max} in nm (log ε): 410 (4.21), 435 (4.06), 551 (3.67), 598 (3.36). FTIR (KBr, cm^{-1}): 3439 (m), 2931 (w), 2894 (w), 2430 (w), 1647.8 (w), 1484 (s), 1431(s), 1369(s), 1280 (m), 1165 (m), 1070 (s), 981 (s), 929 (s), 792 (w), 760 (w).

Synthesis and analytical data of porphyrin derivatives. The 5,10,15,20-tetrakis(pentafluorophenyl)porphyrin ligand **P_1** (Scheme 1 - Via B) was obtained through the condensation of pyrrole with the adequate aldehyde in oxidative acidic conditions [76]. Subsequently, this ligand was structurally modified *via* nucleophilic substitution of one *p*-fluorine atoms by a glycol unit, as described previously [67]. The metallation of the resulting free base porphyrin **P_2** with $Cu(OAc)_2$ afforded the desired copper(II) derivative **Cu-P_2** [63]. Briefly, to a solution of the free base porphyrin **P_2** (0.1 mmol, 50 mg) in $CHCl_3$ (30 mL), a solution of Cu $(OAc)_2$ (1.35 mmol, 270 mg) in MeOH (10 mL) was added. Then, the resulting mixture was refluxed at 70 °C during 24 h under a N_2 atmosphere. After this period, the solvent was evaporated under reduced pressure. Subsequently, the residue was dissolved in $CHCl_3$ (50 mL), and the resulting solution was washed twice with water, dried over anhydrous Na_2SO_4, filtered and concentrated to afford the target compound **Cu-P_2** as a dark red solid in 98 % (46.0 mg) yield.

Analytical data for **Cu-P_2** (**Fig. S3A**): ATR-FTIR (main bands, cm^{-1}): 3439 (m), 2974 (w), 2958 (w), 1743 (w), 1649 (s), 1121 (m), 1019 (s), 916 (s), 810 (s), 732(m), 724 (w). HRMS-ESI(+), $CHCl_3$: *m/z* calculated for $C_{46}H_{14}CuF_{19}N_4O_2$ $(M+H)^+$: 1078.1008; found: 1078.0034. UV–vis (CH_2Cl_2), λ_{max} in nm (log ε): 408 (4.27), 536 (3.62), 571 (3.43).

4.2. Catalytic studies

Oxidation of cyloalkanes. The reactions were carried out in thermostated glass reactors (coated by aluminum foil) coupled with a condenser, in air atmosphere under vigorous stirring at 50 °C. The total reaction volume including all reagents and acetonitrile solvent was 2.5 mL. In a typical procedure, each Cu catalyst (5 μmol) was introduced into CH_3CN solution, followed by the addition of an acid promoter (optional, 50 μmol) and of the gas chromatography (GC) internal standard (CH_3NO_2, 250 μL). Then, each cycloalkane (1.0 mmol) and the oxidant were added. As oxidant, hydrogen peroxide (5.0 mmol, 50 % in H_2O) was typically used, although some tests were also performed with *tert*-butyl hydroperoxide (2.0 mmol, 70 % in H_2O) or *tert*-butyl benzoylperoxide (2.0 mmol, 95 %). The oxidation reactions were followed by withdrawing small aliquots of the reaction mixture at different time periods and analyzed by GC. Prior to GC analyses, the aliquots were treated with an excess of solid PPh_3 for possible reduction of cycloalkyl hydroperoxides (primary products in cycloalkane reactions) and remaining oxidant. In some cases, the aliquots were analyzed twice: before and after the addition of PPh_3. As final oxidation products, cyclic alcohols (e.g., cyclohexanol) and ketones (e.g., cyclohexanone) were detected and quantified by GC and/or GC–MS methods within the studied interval of time. However, at a more prolonged reaction time, some overoxidation products (e.g., cyclic dialcohols and diketones) can be detected in minor amounts. Typical selectivity of the oxidation reactions to the main cyclic alcohol and ketone products was above 95 %.

Carboxylation of alkanes. In a typical procedure, Cu catalyst (5 μmol), H_2O (2.0 mL), CH_3CN (4.0 mL), cycloalkane (1.0 mmol) and $K_2S_2O_8$ (1.50 mmol) were introduced into a stainless steel autoclave (total volume of 20.0 mL). Then, the autoclave was closed, flushed and pressurized with CO (20 atm). The reaction mixture was stirred at 60 °C for 4 h using oil bath and magnetic stirrer. After this period, the autoclave was cooled in an ice bath, degassed, and opened. The reaction mixture was transferred to a glass flask. Et_2O (9.0 mL) and GC internal standard (cycloheptanone or cyclohexanone only in the case of C_7H_{14} carboxylation, 45 μL) were added. After stirring the obtained mixture for 10 min, the aliquots were taken from an organic layer. These were subjected to GC analysis for the quantification (internal standard method) of carboxylic acids as main products; cyclic alcohols and ketones also formed in lower amounts as byproducts of the competing cycloalkane oxidation reactions. No other byproducts were detected within the studied interval of time (4 h). GC peaks were attributed by comparing the obtained chromatograms with those of commercially available samples of products.

Funding

This research work received the support from Fundação para a Ciência e Tecnologia (Portugal), Instituto Superior Técnico, and University of Aveiro.

CRediT authorship contribution statement

Carla I.M. Santos: Writing – original draft, Methodology, Investigation, Conceptualization. **Vitor Rosa:** Methodology, Investigation, Data curation. **M. Graça P.M.S. Neves:** Writing – review & editing, Validation, Methodology, Data curation. **Alexander M. Kirillov:** Writing – review & editing, Visualization, Validation, Investigation. **Marina V. Kirillova:** Writing – review & editing, Writing – original draft, Project administration, Investigation, Data curation, Conceptualization.

Declaration of competing interest

The authors declare that they have no known competing financial interests or personal relationships that could have appeared to influence the work reported in this paper.

Acknowledgments

We are grateful to University of Aveiro, Instituto Superior Técnico (CQE-IST, Portugal), and FCT (Fundação para a Ciência e Tecnologia, Portugal) for research facilities and/or funding trough projects: LA/P/0008/2020, UIDP/50006/2020, PTDC/QUI-QIN/3898/2020, UIDB/00100/2020, UIDP/00100/2020, LA/P/0056/2020, UID/00100/2023, and 2022.05950.PTDC. The Portuguese NMR Network and research contracts REF.IST-ID/95/2018 and 2023.08400.CEECIND (C.I.M. Santos), and CEECIND/03708/2017 (M.V. Kirillova) are acknowledged. We thank Dr. T.A. Fernandes and Dr. A.M.M. Antunes for experimental assistance with mass spectrometry studies. We acknowledge the

MINDlab: Molecular Design & Innovation Laboratory (MINDlab.pt).

Supplementary materials

Supplementary material associated with this article can be found, in the online version, at doi:10.1016/j.mcat.2025.115470.

Data availability

Data will be made available on request.

References

[1] G.D. Yadav, R.K. Mewada, D.P. Wagh, H.G. Manyar, Advances and future trends in selective oxidation catalysis: a critical review, Catal. Sci. Technol. 12 (2022) 7245–7269, https://doi.org/10.1039/D2CY01322C.

[2] L.S. Andrade, H.H.L.B. Lima, C.T.P. Silva, W.L.N. Amorim, J.G.R. Poço, A. López-Castillo, M.V. Kirillova, W.A. Carvalho, A.M. Kirillov, D. Mandelli, Metal–organic frameworks as catalysts and biocatalysts for methane oxidation: the current state of the art, Coord. Chem. Rev. 481 (2023) 215042, https://doi.org/10.1016/j.ccr.2023.215042.

[3] D.L. Nascimento, D. Gygi, M.C. Drummer, M.I. Gonzalez, S.L. Zheng, D.G. Nocera, Photoredox oxidation of alkanes by monometallic copper–oxygen complexes using visible light including one sun illumination, J. Am. Chem. Soc. 146 (2024) 28612–28617, https://doi.org/10.1021/jacs.4c02313.

[4] H. Yang, G. Li, G. Jiang, Z. Zhang, Z. Hao, Heterogeneous selective oxidation over supported metal catalysts: from nanoparticles to single atoms, Appl. Catal. B Environ. 325 (2023) 122384, https://doi.org/10.1016/j.apcatb.2023.122384.

[5] P.J. Figiel, A.M. Kirillov, M.F.C. Guedes da Silva, J. Lasri, A.J.L. Pombeiro, Self-assembled dicopper(II) diethanolaminate cores for mild aerobic and peroxidative oxidation of alcohols, Dalton Trans. 39 (2010) 9879–9888, https://doi.org/10.1039/c0dt00472c.

[6] A.N. Bilyachenko, V.N. Khrustalev, I.S. Arteev, L.S. Shul'pina, N.S. Ikonnikov, M. V. Kirillova, E.S. Shubina, A.M. Kirillov, Y.N. Kozlov, N.N. Lobanov, K.G. Ragimov, D. Sun, Cu_{12}-methylsilsesquioxane cage decorated with $Cu(dppe)_2$ moieties for mild oxidative functionalization of alkanes, Inorg. Chem. 63 (43) (2024) 20404–20414, https://doi.org/10.1021/acs.inorgchem.4c02806.

[7] R. Zhang, Y. Chen, M. Ding, J. Zhao, Heterogeneous Cu catalyst in organic transformations, Nano Res. 15 (2022) 2810–2833, https://doi.org/10.1007/s12274-021-3935-5.

[8] D.J. Fansher, J.N. Besna, A. Fendri, J.N. Pelletier, Choose your own adventure: a comprehensive database of reactions catalyzed by cytochrome P450 BM3 variants, ACS Catal. 14 (2024) 5560–5592, https://doi.org/10.1021/acscatal.4c00086.

[9] M. Lovisari, O.R. Kelly, A.R. McDonald, Hydrocarbon oxidation by a porphyrin-π-cation radical complex, Angew. Chem. Int. Ed. 62 (2023) e202303083, https://doi.org/10.1002/anie.202303083.

[10] H.M. Shen, X. Wang, L. Ning, A.B. Guo, J.H. Deng, Y.B. She, Efficient oxidation of cycloalkanes with simultaneously increased conversion and selectivity using O_2 catalyzed by metalloporphyrins and boosted by $Zn(AcO)_2$: A practical strategy to inhibit the formation of aliphatic diacids, Appl. Catal. A Gen. 609 (2021) 117904, https://doi.org/10.1016/j.apcata.2020.117904.

[11] H.M. Shen, A.B. Guo, Y. Zhang, Q.P. Liu, J.W. Qin, Y.B. She, Relay catalysis of hydrocarbon oxidation using O_2 in the confining domain of 3D metalloporphyrin-based metal–organic frameworks with bimetallic catalytic centers, Chem. Eng. Sci. 260 (2022) 117825, https://doi.org/10.1016/j.ces.2022.117825.

[12] H.M. Shen, X. Wang, H. Huang, Q.P. Liu, D. Lv, Y.B. She, Staged oxidation of hydrocarbons with simultaneously enhanced conversion and selectivity employing O2 as oxygen source catalyzed by 2D metalloporphyrin-based MOFs possessing bimetallic active centers, Chem. Eng. J. 443 (2022) 136126, https://doi.org/10.1016/j.cej.2022.136126.

[13] J.Y. Ni, Y.B. Ding, J. Sun, H.K. Wu, H.M. Shen, Y.B. She, Cycloalkanes oxidation with O_2 catalyzed by a novel metalloporphyrin-based covalent coupling structure with bimetallic catalytic centers through synergistic mode, Catal. Commun. 187 (2024) 106876, https://doi.org/10.1016/j.catcom.2024.106876.

[14] R.D. Teo, J.Y. Hwang, J. Termini, Z. Gross, H.B. Gray, Fighting cancer with corroles, Chem. Rev. 117 (2017) 2711–2729, https://doi.org/10.1021/acs.chemrev.6b00400.

[15] R. Kubba, O.Y. Jyoti, A. Kumar, Phosphorus corroles: synthesis and applications, J. Mol. Struct. 1301 (2024) 137364, https://doi.org/10.1016/j.molstruc.2023.137364.

[16] X. Zhan, D. Kim, Z. Ullah, W. Lee, Z. Gross, D.G. Churchill, Photophysics of corroles and closely related systems for emergent solar energy, medicinal, and materials science applications, Coord. Chem. Rev. 495 (2023) 215363, https://doi.org/10.1016/j.ccr.2023.215363.

[17] W. Deng, M. Jia, Q. Shi, Y. Xu, Y. Feng, Y. Zhao, M. Gong, B. Zhang, A unique corrole-based metal–organic polymer for synergistic phototherapy, Mater. Chem. Front. 8 (2024) 575–584, https://doi.org/10.1039/D3QM01056B.

[18] A. Mahammed, Z. Gross, Milestones and Most recent advances in corrole's science and technology, J. Am. Chem. Soc. 145 (23) (2023) 12429–12445, https://doi.org/10.1021/jacs.3c00282.

[19] H. Moon, G.-J. Jeong, T.S. Reddy, D.H. Yang, M.S. Choi, Porphyrin-based fluorescent probes for imaging mitochondria in living cells, Dyes Pigm. 231 (2024) 112369, https://doi.org/10.1016/j.dyepig.2024.112369.

[20] G. Lu, S. Ding, S. Meng, Y. Zhang, A near-infrared turn-on fluorescent probe for specific detection of cysteine and its application based on a corrole fluorophore, Dyes Pigm. 227 (2024) 112194, https://doi.org/10.1016/j.dyepig.2024.112194.

[21] J. Bai, R. Li, J. Huang, X. Shang, G. Wang, S. Chao, Metal-free corrole-based donor–acceptor porous organic polymers as efficient bifunctional catalysts for hydrogen evolution and oxygen reduction reactions, Inorg. Chem. Front. 11 (16) (2024) 5091–5102, https://doi.org/10.1039/D4QI00862F.

[22] M.K. Chahal, Advances in the use of metal-free tetrapyrrolic macrocycles as catalysts, Beilstein J. Org. Chem. 20 (2024) 3085–3112, https://doi.org/10.3762/bjoc.20.257.

[23] A.B. Guo, J.W. Qin, K.K. Wang, Q.P. Liu, H.K. Wu, M. Wang, H.M. Shen, Y.B. She, Synergetic catalytic oxidation of C–H bonds in cycloalkanes and alkyl aromatics by dimetallic active sites in 3D metalloporphyrinic MOFs employing O_2 as oxidant with increased conversion and unconsumed selectivity, Mol. Catal. 535 (2023) 112853, https://doi.org/10.1016/j.mcat.2022.112853.

[24] H.M. Shen, L. Zhang, J.H. Deng, J. Sun, Y.B. She, Enhanced catalytic performance of porphyrin cobalt(II) in the solvent-free oxidation of cycloalkanes (C5–C8) with molecular oxygen promoted by porphyrin zinc(II), Catal. Commun. 132 (2019) 105809, https://doi.org/10.1016/j.catcom.2019.105809.

[25] S. Payamifar, M. Abdouss, A.P. Marjani, An overview of porphyrin-based catalysts for sulfide oxidation reactions, Polyhedron 269 (2025) 117389, https://doi.org/10.1016/j.poly.2025.117389.

[26] X. Lu, X. Niu, J. Qi, Q. Wei, Z. Ji, J. Lan, S. Wang, Iron porphyrin as a cytochrome P450 model for the oxidation of xanthene, J. Organomet. Chem. 1021 (2024) 123371, https://doi.org/10.1016/j.jorganchem.2024.123371.

[27] R.M.S. Junior, E.H. Santos, S. Nakagaki, Metalloporphyrin-based multifunctional catalysts for one-pot assisted tandem reaction, Mol. Catal. 541 (2023) 113080, https://doi.org/10.1016/j.mcat.2023.113080.

[28] K.A.D.F. Castro, F.H.C. Lima, M.M.Q. Simões, M.G.P.M.S. Neves, F.A.A. Paz, R. F. Mendes, S. Nakagaki, J.A.S. Cavaleiro, Synthesis, characterization and catalytic activity under homogeneous conditions of ethylene glycol substituted porphyrin manganese(III) complexes, Inorg. Chim. Acta 455 (2) (2017) 575–583, https://doi.org/10.1016/j.ica.2016.05.038.

[29] K.A.D.F. Castro, K.C.M. Westrup, S. Silva, P.M.R. Pereira, M.M.Q. Simões, M.G.P. M.S. Neves, J.A.S. Cavaleiro, J.P.C. Tomé, S. Nakagaki, Iron(III) complexation with galactodendritic porphyrin species and hydrocarbons' oxidative transformations, Eur. J. Inorg. Chem. 2021 (28) (2021) 2857–2869, https://doi.org/10.1002/ejic.202100359.

[30] J.F. Stival, C.N. Cechin, B.A. Iglesias, E.S. Lang, J.S. Rebouças, S. Nakagaki, ZnO with different morphologies sensitized by metalloporphyrins as catalysts for H_2 production by water splitting under sunlight, Chem. Asian J. 20 (1) (2025) e202580102, https://doi.org/10.1002/asia.202580102.

[31] J.T. Groves, T.E. Nemo, R.S. Myers, Hydroxylation and epoxidation catalyzed by iron-porphine complexes. Oxygen transfer from iodosylbenzene, J. Am. Chem. Soc. 101 (4) (1979) 1032–1033, https://doi.org/10.1021/ja00498a040.

[32] F. Li, Y. Li, Y. Wan, H. Lv, X. Gao, Y. Yu, Metalloporphyrin-based biomimetic catalysis: applications, modifications and flexible microenvironment influences (a review), Russ. J. Gen. Chem. 93 (1) (2023) 189–214, https://doi.org/10.1134/S1070363223010255.

[33] Z. Ren, K. Gong, B. Zhao, S.L. Chen, J. Xie, Boosting the catalytic performance of metalloporphyrin-based covalent organic frameworks via coordination engineering for CO_2 and O_2 reduction, Mater. Chem. Front. 8 (2024) 1958–1970, https://doi.org/10.1039/D3QM01315D.

[34] S.H. El-Khalafy, M.T. Hassanein, M.M. Alaskary, N.A. Salahuddin, Synthesis and characterization of Co(II) porphyrin complex supported on chitosan/graphene oxide nanocomposite for efficient green oxidation and removal of Acid Orange 7 dye, Sci. Rep. 14 (1) (2024) 17073, https://doi.org/10.1038/s41598-024-65517-z.

[35] I. Ahmad, S.R. Shagufta, Metal-porphyrin in epoxidation of olefins: recent advances, Tetrahedron 104 (2022) 132604, https://doi.org/10.1016/j.tet.2021.132604.

[36] C.K. Chang, M.S. Kuo, Reaction of iron(III) porphyrins and iodosoxylene. The active oxene complex of cytochrome P-450, J. Am. Chem. Soc. 101 (12) (1979) 3413–3415, https://doi.org/10.1021/ja00506a063.

[37] E. Tabor, J. Połtowicz, K. Pamin, S. Basąg, W. Kubiak, Influence of substituents in meso-aryl groups of iron μ-oxo porphyrins on their catalytic activity in the oxidation of cycloalkanes, Polyhedron 119 (2016) 342–349, https://doi.org/10.1016/j.poly.2016.08.048.

[38] Z. Feng, Y. Xie, F. Hao, P. Liu, H.A. Luo, Catalytic oxidation of cyclohexane to KA oil by zinc oxide supported manganese 5,10,15,20-tetrakis(4-nitrophenyl) porphyrin, J. Mol. Catal. A: Chem. 410 (2015) 221–225, https://doi.org/10.1016/j.molcata.2015.09.027.

[39] V.S. Da Silva, S. Nakagaki, G.M. Ucoski, Y.M. Idemori, G.F. Silva, New highly brominated Mn-porphyrin: a good catalyst for activation of inert C–H bonds, RSC Adv. 5 (2015) 106589–106598, https://doi.org/10.1039/C5RA20690A.

[40] A.R. Antonangelo, K.C.M. Westrup, L.A. Burt, C.G. Bezzu, T. Malewschik, G. S. Machado, F.S. Nunes, N.B. McKeown, S. Nakagaki, Synthesis, crystallographic characterization and homogeneous catalytic activity of novel unsymmetric porphyrins, RSC Adv. 7 (80) (2017) 50610–50618, https://doi.org/10.1039/C7RA08734A.

[41] A.R. Antonangelo, C.G. Bezzu, N.B. McKeown, S. Nakagaki, Highly active manganese porphyrin-based microporous network polymers for selective oxidation reactions, J. Catal. 369 (2019) 133–142, https://doi.org/10.1016/j.jcat.2018.10.036.

[42] M.M. Pereira, L.D. Dias, M.J.F. Calvete, Metalloporphyrins: bioinspired oxidation catalysts, ACS Catal. 8 (11) (2018) 10784–10808, https://doi.org/10.1021/acscatal.8b01871.
[43] V.H.A. Pinto, J.S. Rebouças, G.M. Ucoski, E.H. de Faria, B.F. Ferreira, R. Gil, S. Nakagaki, Mn porphyrins immobilized on non-modified and chloropropyl-functionalized mesoporous silica SBA-15 as catalysts for cyclohexane oxidation, Appl. Catal. A Gen. 526 (2016) 9–20, https://doi.org/10.1016/j.apcata.2016.07.018.
[44] R. Hajian, E. Bahrami, Mn(III)-porphyrin immobilized on the graphene oxide–magnetite nanocomposite as an efficient heterogeneous catalyst for the epoxidation of alkenes, Catal. Lett. 152 (2022) 2445–2456, https://doi.org/10.1007/s10562-021-03827-x.
[45] K.M. Mantovani, K.C.M. Westrup, R.M. da Silva Junior, S. Jaerger, F. Wypych, S. Nakagaki, Oxidation catalyst obtained by the immobilization of layered double hydroxide/Mn(III) porphyrin on monodispersed silica spheres, Dalton Trans. 47 (9) (2018) 3068–3073, https://doi.org/10.1039/C7DT03656F.
[46] L.Q. Mo, X.F. Huang, G. Huang, G.P. Yuan, S.J. Wei, Highly active catalysis of cobalt tetrakis(pentafluorophenyl)porphyrin promoted by chitosan for cyclohexane oxidation in response-surface-methodology-optimized reaction conditions, ChemistryOpen 8 (1) (2019) 104–113, https://doi.org/10.1002/open.201800268.
[47] J.I.T. Costa, A.T. Tomé, M.G.P.M.S. Neves, J.A.S. Cavaleiro, 5,10,15,20-Tetrakis (pentafluorophenyl)porphyrin: a versatile platform to novel porphyrinic materials, J. Porphyr. Phthalocyanines 15 (11–12) (2011) 1116–1133, https://doi.org/10.1142/S1088424611004294.
[48] M.M.Q. Simões, N.M.M. Moura, K.A.D.F. Castro, S.L.H. Rebelo, M.G.P.M.S. Neves, J.A.S. Cavaleiro, A.J.L. Pombeiro, Metalloporphyrins as oxidative catalysts: synthesis of high-value-added compounds, Eds., in: A.J.L. Pombeiro, K. T. Mahmudov, M.F.C. Guedes da Silva (Eds.), Synthesis and Applications in Chemistry and Materials, World Scientific, Singapore, 2024, pp. 79–109, https://doi.org/10.1142/9789811283215_0015.
[49] A.R. Antonangelo, C.G. Bezzu, S.S. Mughal, T. Malewschik, N.B. McKeown, S. Nakagaki, A porphyrin-based microporous network polymer that acts as an efficient catalyst for cyclooctene and cyclohexane oxidation under mild conditions, Catal. Commun. 99 (2017) 100–104, https://doi.org/10.1016/j.catcom.2017.05.024.
[50] Y. Yang, P. Yan, D. Wang, F. Xie, D. Song, N. Wang, J. Li, A2B2-zinc(II)porphyrin/divinylbenzene copolymer as efficiently bifunctional catalyst for cycloaddition of CO_2 with epoxides, Eur. J. Inorg. Chem. 28 (1) (2025) e202400589, https://doi.org/10.1002/ejic.202400589.
[51] A.N. Biswas, A. Pariyar, S. Bose, P. Das, P. Bandyopadhyay, Mild oxidation of hydrocarbons catalyzed by iron corrole with tert-butylhydroperoxide, Catal. Commun. 11 (2010) 1008–1011, https://doi.org/10.1016/j.catcom.2010.05.006.
[52] A. Mahammed, Z. Gross, Milestones and most recent advances in corrole's science and technology, J. Am. Chem. Soc. 145 (2023) 12429–12445, https://doi.org/10.1021/jacs.3c00282.
[53] S. Nakagaki, C.R. Xavier, A.J. Wosniak, A.S. Mangrich, F. Wypych, M.P. Cantão, I. Denicoló, L.T. Kubota, Synthesis and characterization of zeolite-encapsulated metalloporphyrins, Colloids Surf. A Physicochem. Eng. Asp. 168 (2000) 261–276, https://doi.org/10.1016/S0927-7757(99)00503-8.
[54] H.M. Shen, A.B. Guo, Y. Zhang, Q.P. Liu, J.W. Qin, Y.B. She, Relay catalysis of hydrocarbon oxidation using O_2 in the confining domain of 3D metalloporphyrin-based metal-organic frameworks with bimetallic catalytic centers, Chem. Eng. Sci. 260 (2022) 117825, https://doi.org/10.1016/j.ces.2022.117825.
[55] A.B. Guo, J.W. Qin, K.K. Wang, Q.P. Liu, H.K. Wu, M. Wang, H.M. Shen, Y.B. She, Synergetic catalytic oxidation of C–H bonds in cycloalkanes and alkyl aromatics by dimetallic active sites in 3D metalloporphyrinic MOFs employing O_2 as oxidant with increased conversion and unconsumed selectivity, Mol. Catal. 535 (2023) 112853, https://doi.org/10.1016/j.mcat.2022.112853.
[56] X.Y. Zhou, B. Fu, W.D. Jin, X. Wang, K.K. Wang, M. Wang, Y.B. She, H.M. Shen, Efficient and Selective oxygenation of cycloalkanes and alkyl aromatics with Oxygen through synergistic catalysis of bimetallic active centers in two-dimensional metal-organic frameworks based on metalloporphyrins, Biomimetics 8 (2023) 325, https://doi.org/10.3390/biomimetics8030325.
[57] M.V. Kirillova, C.I.M. Santos, V. André, T.A. Fernandes, S.S.P. Dias, A.M. Kirillov, Self-assembly generation, structural features, and oxidation catalytic properties of new aqua-soluble copper(II)–aminoalcohol derivatives, Inorg. Chem. Front. 4 (2017) 968–977, https://doi.org/10.1039/C6QI00553E.
[58] K.I. Trusau, M.V. Kirillova, V. André, A.I. Usevich, A.M. Kirillov, Mild oxidative functionalization of cycloalkanes catalyzed by novel dicopper(II) cores, Mol. Catal. 503 (2021) 111401, https://doi.org/10.1016/j.mcat.2021.111401.
[59] I.F.M. Costa, M.V. Kirillova, V. André, T.A. Fernandes, A.M. Kirillov, Time-dependent self-assembly of copper(ii) coordination polymers and tetranuclear rings: catalysts for oxidative functionalization of saturated hydrocarbons, Inorg. Chem. 60 (2021) 14491–14503, https://doi.org/10.1021/acs.inorgchem.1c01268.
[60] K.A.D.F. Castro, M.M.Q. Simões, M.G.P.M.S. Neves, J.A.S. Cavaleiro, R.R. Ribeiro, F. Wypych, S. Nakagaki, Synthesis of new metalloporphyrin derivatives from [5,10,15,20-tetrakis(pentafluorophenyl)porphyrin] and 4-mercaptobenzoic acid for homogeneous and heterogeneous catalysis, Appl. Catal. A Gen. 503 (2015) 9–19, https://doi.org/10.1016/j.apcata.2014.12.048.
[61] L.D. Dias, F.M.S. Rodrigues, M.J.F. Calvete, S.A.C. Carabineiro, M.D. Scherer, A.R. L. Caires, J.G. Buijnsters, J.L. Figueiredo, V.S. Bagnato, M.M. Pereira, Porphyrin–nanodiamond hybrid materials—active, stable and reusable cyclohexene oxidation catalysts, Catalysts 10 (2020) 1402, https://doi.org/10.3390/catal10121402.
[62] K.A.D.F. Castro, J.M.M. Rodrigues, R.F. Mendes, M.G.P.M.S. Neves, M.M. Q. Simões, J.A.S. Cavaleiro, F.A. Almeida Paz, J.P.C. Tomé, S. Nakagaki, New copper porphyrins as functional models of catechol oxidase, J. Catal. 344 (2016) 303–312, https://doi.org/10.1016/j.jcat.2016.09.010.
[63] K.A.D.F. Castro, F. Figueira, R.F. Mendes, J.A.S. Cavaleiro, M.G.P.M.S. Neves, M.M. Q. Simões, F.A. Almeida Paz, J.P.C. Tomé, S. Nakagaki, Copper–Porphyrin–metal–organic frameworks as oxidative heterogeneous catalysts, ChemCatChem 9 (2017) 2939–2945, https://doi.org/10.1002/cctc.201700484.
[64] S. Nardis, F. Mandoj, M. Stefanelli, R. Paolesse, Metal complexes of corrole, Coord. Chem. Rev. 388 (2019) 360–405, https://doi.org/10.1016/j.ccr.2019.02.034.
[65] J.L. Sessler, E. Tomat, Transition-metal complexes of expanded porphyrins, Acc. Chem. Res. 40 (2007) 371–379, https://doi.org/10.1021/ar600006n.
[66] C.I.M. Santos, L. Rodríguez-Pérez, G. Gonçalves, S.N. Pinto, M. Melle-Franco, P.A. A.P. Marques, M.A.F. Faustino, M.Á. Herranz, N. Martin, M.G.P.M.S. Neves, J.M. G. Martinho, E.M.S. Maçôas, Novel hybrids based on graphene quantum dots covalently linked to glycol corroles for multiphoton bioimaging, Carbon 166 (2020) 164–174, https://doi.org/10.1016/j.carbon.2020.04.012.
[67] C.I.M. Santos, G. Gonçalves, M. Cicuéndez, I. Mariz, V.S. Silva, H. Oliveira, F. Campos, S.I. Vieira, P.A.A.P. Marques, E.M.S. Maçôas, M.G.P.M.S. Neves, J.M. G. Martinho, Biocompatible hybrids based on nanographene oxide covalently linked to glycolporphyrins: Synthesis, characterization and biological evaluation, Carbon 135 (2018) 202–214, https://doi.org/10.1016/j.carbon.2018.04.040.
[68] M.V. Kirillova, A. Pastor, A.M. Kirillov, Multimetal layered double hydroxides: synthesis, characterization, and synergic effect in mild catalytic oxidation of alkanes, Inorg. Chem. 64 (17) (2025) 8668–8677, https://doi.org/10.1021/acs.inorgchem.5c00461.
[69] Y. Li, S. Chen, Y. Jin, X. Li, R. Zhang, R. Liu, The role of V-species and O-species on controlled-hydrogen-reduction VOx surfaces in cyclohexane oxidation, ChemistrySelect 8 (29) (2023) e202301223, https://doi.org/10.1002/slct.202301223.
[70] N. Carnieri, A. Harriman, G. Porter, K. Kalyanasundaram, Photochemistry of manganese porphyrins. Part 7. characterisation of manganese porphyrins in organic and aqueous/organic microheterogeneous systems, J. Chem. Soc. Dalton Trans. 7 (1982) 1231–1238, https://doi.org/10.1039/DT9820001231.
[71] K. Ogawa, Y. Umetsu, K. Kamimura, Changes in the absorption spectra and colour of tetraphenylporphyrins after redox reactions, J. Chem. Res. 44 (2020) 613, https://doi.org/10.1177/1747519820910915.
[72] U. Schuchardt, D. Cardoso, R. Sercheli, R. Pereira, R.S. Da Cruz, M.C. Guerreiro, D. Mandelli, E.V. Spinacé, E.L. Pires, Cyclohexane oxidation continues to be a challenge, Appl. Catal. A Gen. 211 (2001) 1–17, https://doi.org/10.1016/S0926-860X(01)00472-0.
[73] M.N. Kopylovich, A.M. Kirillov, A.K. Baev, A.J.L. Pombeiro, Heteronuclear iron (III)–chromium(III) hydroxo complexes and hydroxides, and their catalytic activity towards peroxidative oxidation of alkanes, J. Mol. Catal. A Chem. 206 (2003) 163–178, https://doi.org/10.1016/S1381-1169(03)00420-5.
[74] D.T. Gryko, B. Koszarna, Refined methods for the synthesis of meso-substituted A_3- and trans-A_2B-corroles, Org. Biomol. Chem. 1 (2003) 350–357, https://doi.org/10.1039/B208950E.
[75] C.I.M. Santos, M. Cicuéndez, G. Gonçalves, L. Rodríguez-Pérez, M.T. Portolés, M.A. F. Faustino, M.Á. Herranz, M.G.P.M.S. Neves, J.M.G. Martinho, E.M.S. Maçôas, N. Martín, Safety assessment of new nanodiamonds@corrole hybrids addressed by the response of RAW-264.7 macrophages, J. Mater. Chem. B 11 (2023) 675–686, https://doi.org/10.1039/D2TB01863B.
[76] K.A.D.F. Castro, M.M.Q. Simões, M.G.P.M.S. Neves, J.A.S. Cavaleiro, F. Wypych, S. Nakagaki, Glycol metalloporphyrin derivatives in solution or immobilized on LDH and silica: synthesis, characterization and catalytic features in oxidation reactions, Catal. Sci. Technol. 4 (2014) 129–141, https://doi.org/10.1039/C3CY00472D.